

ОБЪЕДИНЕННЫЙ
ИНСТИТУТ
ЯДЕРНЫХ
ИССЛЕДОВАНИЙ
ДУБНА



2/11-74

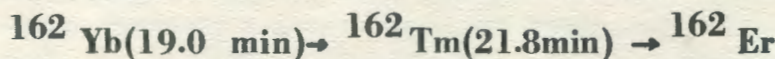
44-22

E6 - 8008

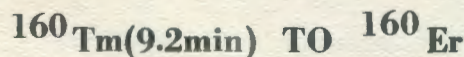
3464/2-74

A.A.Abdurazakov, G.Beyer, K.Ya.Gromov,
E.Herrmann, T.A.Islamov, M.Jachim, F.Molnar,
G.Musiol, H.-U.Siebert, H.Strusny, H.Tyroff,
S.A.Usmanova

THE DECAY CHAIN



AND THE DECAY OF

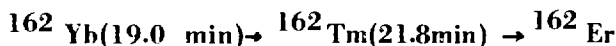


1974

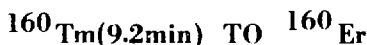
ЛАБОРАТОРИЯ ЯДЕРНЫХ ПРОБЛЕМ

A.A.Abdurazakov,¹ G.Beyer,² K.Ya.Gromov,
 E.Herrmann,⁶ T.A.Islamov,¹ M.Jachim,³ F.Molnar,⁷
 G.Musiol,⁶ E.-U.Siebert,⁴ H.Strusny,⁵ H.Tyroff,⁵
 S.A.Usmanova

THE DECAY CHAIN



AND THE DECAY OF



Submitted to Czechoslovak Journal
 of Physics

¹ On leave from the University Tashkent, USSR.

² On leave from ZfK Rossendorf/Dresden, DDR.

³ On leave from the Ústav Jaderných Výskumu, Řež u Prahy, CSSR.

⁴ On leave from the Technical University, Dresden, DDR.

⁵ Zentralinstitut für Kernforschung, Rossendorf/Dresden, DDR.

⁶ Technische Universität Dresden, DDR.

⁷ MTA Központi Fizikai Kutató Intézet, Budapest, Hungary.

1. Introduction

In recent works on the ^{162}Tm level scheme (refs. ^{1,2}) the 1^- (ground-state (g.s.)) and 2^- (44.64 keV) members of the $K=1$ ground-state band and a two-quasiparticle state 1^+ , p7[2⁻1523]-n5[2⁻1523] (163.36 keV) were identified.

The level scheme of ^{162}Er has been studied by several authors. Members of the $K=0$ ground-state band were found up to spin 20 (ref. ³), of the γ -vibrational band up to spin 4 (refs. ¹⁻⁶), of the β -vibrational band up to spin 4 (ref. ¹) and several unidentified high-lying states (refs. ¹⁻⁶).

No detailed investigation of the ^{160}Tm decay has been performed previously. The existence of a 9.2 min ^{160}Tm activity was reported by Neiman and Ward ⁷ and de Boer et al. ⁸. A ^{160}Tm decay scheme involving the 0^+ (g.s.), 4^+ (126.1 keV) and 1^+ (390.3 keV) members of the $K=0$ ground-state band ³ and two unidentified levels at 853.5 and 926.4 keV in ^{160}Er has been proposed by de Boer et al. ⁸

Spins of $I=1$ for the ground-states of ^{162}Tm and ^{160}Tm and of $I=0$ for the ^{160}Er ground-state were measured with an atomic beam technique by Ekstrom et al. ⁹⁻¹¹.

The present investigations were undertaken to study the levels in ^{162}Tm , ^{162}Er and ^{160}Er by electron capture and positron decay spectroscopy with $\text{Ge}(\text{Li})$ and $\text{Si}(\text{Li})$ detectors and magnetic β -spectrographs. The singles γ -ray spectrum, the conversion electron spectrum, the positron spectrum, γ - γ and β - γ coincidences were measured.

Preliminary results of the present investigations of the decay of ^{162}Yb (refs. ^{1,12,13}), ^{162}Tm (refs. ^{1,12}) and ^{160}Tm (refs. ¹⁴⁻¹⁶) have been published previously.

2. Experimental Details and Results

2.1. Source production

The activities of ^{162}Yb , ^{162}Tm and ^{160}Tm were produced by the spallation reaction induced by high energy protons on a tantalum target. Suspensions of about 3g Ta_2O_5 in 3 ml 0.1M HNO_3 were irradiated for 20 min in the external 660 MeV proton beam of the Dubna synchrocyclotron with a current of $0.1\mu\text{A}$. Because of the high recoil energy of the spallation products about 40% of the products are stabilised in the liquid phase and can easily be separated from the target material by filtration ¹⁷. During 1 minute the rare earth spallation products were absorbed from the filtrate at a small amount of cation exchange resin (10 mg) with a yield better than 80%. After washing the resin with 0.1M NH_4Cl solution and water the rare earth spallation products were separated by cation exchange chromatography at a 2.6×60 mm column filled with Aminex A5. By elution with 0.08 M α -oxy-iso-butyric acid (α -HIB) of the value $\text{pH} = 4.8$ the Yb and Tm fractions appeared after elution of the Lu fraction in a volume of 1-2 drops about 10 min after the end of irradiation. The Yb and Tm fractions were evaporated until dryness at a platinum foil. After adding of 0.02 ml of 2.10^{-3} M α -HIB the Yb and Tm activities were deposited as hydroxide by electrolysis on a 5 mm^2 tungsten foil. Use of 30 seconds for electrolysis (75V, 2.5 mA/mm^2) gives the yield better than 80%. By heating the foil up to 500°C the Yb and Tm hydroxide were transformed to Yb and Tm oxide.

After this chemical process the Yb and Tm isotope separations were performed using an electromagnetic mass-separator ¹⁸ with a pipe-type surface ionization source ¹⁹. The separation efficiency has been

measured to be about 30% for a 5 min separation time. All separated samples were collected on aluminized polyester tapes. The spot on which the activity was concentrated was about 1-2 mm across. The distance between neighbouring masses was 18 mm. The isotopic admixture did not exceed 0.1%. About 20 min after the end of irradiation the measurements of the samples were started.

The experimental methods for the production of the β -spectrograph sources applied to measure the conversion electron spectra have been described elsewhere^[20,21] and therefore only a summary is given here. A metallic tantalum target was irradiated for 30-60 min on the internal 680 MeV proton beam (current $2.3 \mu A$) of the Dubna synchrocyclotron. The Yb and Tm activities were chemically separated from the other spallation products^[20] and were then deposited by electrolysis on a $50 \mu m$ platinum wire^[21]. The measurements of those conversion electron sources were started about 1 hour after the end of irradiation.

2.2. Gamma-ray singles measurements

For the measurements of singles γ -ray spectra Ge(Li) detectors of volumes 27 and $38 cm^3$ with a system resolution for ^{60}Co of 3.5 keV and Ge(Li) detectors of volumes 2.4 and $1 cm^3$ with a system resolution for ^{57}Co of 0.6 keV were used. The efficiency and energy calibration of the Ge(Li) detectors were performed with γ -rays from the sources ^{51}Mn , ^{56}Co , ^{60}Co , ^{75}Sn , ^{110m}Ag , ^{133}Ba , ^{137}Cs , ^{152}Eu , ^{182}Ta , ^{207}Bi , ^{226}Ra and ^{241}Am .

The high energy range of the γ -ray spectra of the ^{162}Tm and ^{160}Tm activities was measured using an absorber of 3 mm Pb + 1 mm Cd + 1 mm Cu. In order to improve the statistical accuracy the spectra from up to 10 sources were added. The energy values of the high energy transitions in the ^{162}Tm decay were determined in a special calibration experiment by measuring the γ -ray spectrum of the ^{162}Tm activity simultaneously with source of ^{56}Co , ^{60}Co and ^{110m}Ag .

In order to determine the intensity of the annihilation radiation in the decays of ^{162}Yb , ^{162}Tm and ^{160}Tm the sources were sandwiched between 3 mm thick Copper plates. The efficiency for the detection of the annihilation radiation was determined with ^{22}Na source measured in the same position as the ^{162}Yb , ^{162}Tm and ^{160}Tm sources.

All spectra were stored in several 4096 channel memories, recorded on magnetic tape and analysed by means of light pen systems and computers^{22,23}.

The low energy part of the ^{162}Yb γ -ray spectrum measured with the 2.4 cm³ Ge(Li) detector is shown in fig. 1. In figs. 2 and 3 the medium and high energy ranges of the ^{162}Tm and ^{160}Tm γ -ray spectra measured by means of the 38 cm³ Ge(Li) detector are plotted.

The results of singles γ -ray measurements of the ^{162}Yb , ^{162}Tm and ^{160}Tm decay are listed in tables 1, 2 and 3. For the normalization of the γ -ray intensities the sum of the intensities of electron capture and positron decay for each of these nuclides was assumed to be 100 decays. The intensity of the electron capture branch was obtained from the measured KX-ray intensity corrected for the contribution of the internal conversion of the γ -ray transitions, the fluorescent yield ($\omega_K = 0.93$ (ref. 21)) and the L and M capture ($(\epsilon_L + \epsilon_M)/\epsilon_K \approx 0.17$ (ref. 21)). The positron intensity was derived from the measured intensity of the annihilation radiation (see tables 1, 2 and 3).

3, 134 and 39 new γ -rays were observed in the decays of ^{162}Yb , ^{162}Tm and ^{160}Tm , respectively (see tables 1, 2 and 3).

2.3. Conversion electron measurements

The conversion electron measurements were performed with the aid of magnetic β -spectrographs with the high resolution of 0.05% ref. 25. Electrons were recorded on photo plates of NIKFI-R-50 μ type. The intensities of the lines were evaluated from the peak areas of the

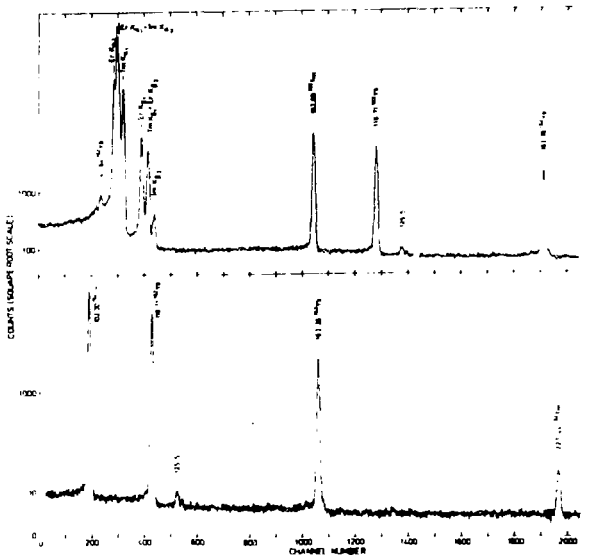


Fig. 1. Low energy part of the ^{162}Yb γ -ray spectrum measured with the 2.4 cm^3 Ge(Li) detector. (The 125.5keV γ -ray transition was not identified).

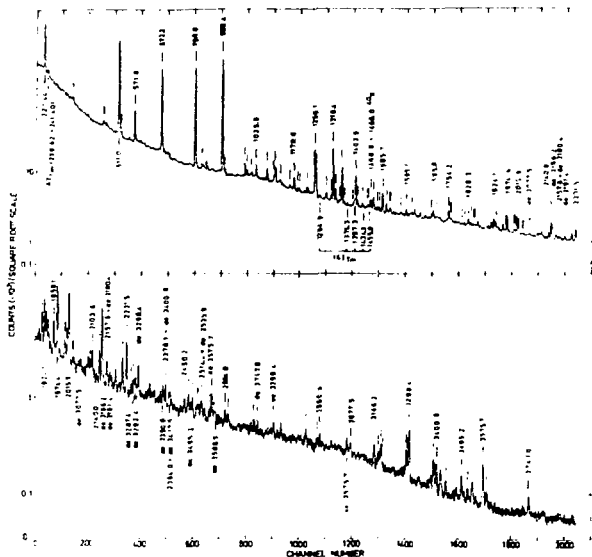


Fig. 2. High energy range of ^{162}Tm γ -ray spectrum measured by means of the $38\text{ cm}^3\text{ Ge(Li)}$ detector with the absorber of 3 mm Pb + 1 mm Cd + 1 mm Cu. The ^{162}Tm lines are indicated by vertical strokes and partly by their energy values given in keV. Other lines are marked by the symbol of their mother nuclei.

Table 1 Energies and intensities of the γ -ray transitions in the decay ^{162}Yb (EC) ^{162}Tm

E_{γ} , keV	I_{γ}	I_{K}	I_{111}	I_{1111}	I_{11111}	Multi-polarity
KX (Tm)	50 ± 16					
44.04 ± 0.02 ^{a),b)}	3.0 ± 0.8		16.0	10.5	14.0	M1+7% E2
115.74 ± 0.02 ^{a)}	28.2 ± 3.0	6.1	0.7	0.12	0.17	E1
163.76 ± 0.04 ^{a)}	39.7 ± 4.0 ^{b)}	1.0 ^{b)}	0.4	0.07	0.08	E1
511.0 ^{c)}	$4 (2 \times 2)$					
575.7 ± 0.7	3.2 ± 0.8					
607.0 ± 0.7	2.4 ± 0.7					
618.5 ± 0.9	4 ± 1.5					

a) γ -ray transition observed in refs. [1,2].

b) Normalization values.

c) Annihilation radiation.

d) Experimental M-subshell ratios of the 44.04 keV transition were determined to be $M_1/M_{111}/M_{1111} = 4.0/1.0/0.7$

All intensities are given per 100 decays (see text). The errors of the conversion electron intensities are of the order of 20%.

Table 2 Energies and intensities of the J -ray transition in the decay $^{162}\text{Tm}(\text{J})^{162}\text{Er}$

E_J , keV	I_J ^{d)}	E_J , keV	I_J ^{d)}
KX (Er)	92 ±16	1318.4±0.3 ^{a,b)}	5.1±0.5
102.00 ±0.05 ^{a,b)}	17.3±2.0	1328.1±0.4	1.0±0.1
227.44 ±0.07 ^{a,b)}	6.3±0.5	1345.8±0.7	0.4±0.1
337.0 ±0.8	≈ 0.3	1352.0±0.3 ^{b)}	3.6±0.3
452.3 ±0.6 ^{b)}	0.2±0.1	1371.1±0.5	0.2±0.1
456.7 ±0.6	0.2±0.1	1394.5±0.8	≈ 0.1
465.0 ±0.6	0.2±0.1	1403.9±0.3 ^{b)}	2.8±0.3
511.0 ^{f)}	2x(6.4±0.9)	1411.8±0.4	0.4±0.1
510.3 ±0.6 ^{b)}	0.5±0.2	1429.7±0.5	0.3±0.1
511.0 ±0.3 ^{a,b,c)}	2.1±0.2	1447.0±0.7	0.2±0.1
672.2 ±0.3 ^{a,b,c)}	0.2±0.5	1450.9±0.5	0.2±0.1
708.8 ±0.3 ^{a,b,c)}	8.7±0.7	1460.8±0.7	≈ 0.2
821.4 ±0.7	0.2±0.1	1470.7±0.4 ^{b)}	1.0±0.1
831.0 ±0.7	0.2±0.1	1486.3±0.6	0.3±0.1
841.1 ±0.4 ^{b)}	0.6±0.1	1493.3±0.5 ^{b)}	0.3±0.1
900.4 ±0.3 ^{a,b,c)}	11.6±1.0	1505.7±0.4 ^{b)}	1.8±0.2
909.8 ±0.3	0.3±0.1	1520.7±0.5	0.8±0.1
985.0 ±0.4 ^{b)}	1.1±0.1	1533.6±0.6	0.3±0.1
993.4 ±0.4	0.6±0.1	1536.7±0.6	0.3±0.1
1010.2 ±0.5	0.4±0.1	1548.6±0.6	0.3±0.1
1026.9 ±0.4 ^{b)}	1.0±0.1	1556.8±0.7	0.2±0.1
1064.8 ±0.4 ^{b)}	1.1±0.1	1573.9±0.7	0.2±0.1
1095.5 ±0.5	0.4±0.1	1595.1±0.5 ^{b)}	0.4±0.1
1099.9 ±0.4	1.2±0.2	1616.2±0.6	0.3±0.1
1117.9 ±0.6	0.2±0.1	1627.0±0.5	0.6±0.1
1155.1 ±0.6	0.2±0.1	1647.7±0.5	0.3±0.1
1170.8 ±0.4 ^{b)}	1.0±0.1	1660.7±0.6	0.2±0.1
1185.1 ±0.6	0.2±0.1	1690.1±0.7	0.2±0.1
1193.2 ±0.6	0.2±0.1	1695.8±0.5	0.7±0.1
1221.4 ±0.5	0.5±0.1	1754.2±0.5	0.9±0.1
1250.1 ±0.3 ^{a,b)}	4.5±0.5	1759.2±0.7	0.2±0.1
1254.5 ±0.4	1.8±0.2	1763.2±0.8	0.2±0.1
1293.2 ±0.5	0.5±0.1	1806.0±0.8	0.2±0.1
1310.3 ±0.5	0.4±0.1	1814.3±0.6	0.3±0.1
		1828.3±0.5	0.6±0.1

Table 2 (continued)

E_j , keV	I_j ^{d)}	E_j , keV	I_j ^{d)}
1838.3±0.6	0.3±0.1	2358.0±1.0	≈ 0.1
1847.7±0.5	0.2±0.1	2378.1±0.7	≈ 0.2
1852.2±0.5	0.2±0.1	2394.0±1.0	0.4±0.1
1864.1±0.6	0.7±0.1	2396.0±1.0	0.2±0.1
1874.5±0.8	0.3±0.1	2450.2±0.7	0.2±0.1
1914.6±0.5	0.6±0.1	2464.9±0.7	0.3±0.1
1924.1±0.5	0.5±0.1	2481.1±0.9	0.2±0.1
1931.3±0.5	0.7±0.1	2497.5±0.8	0.2±0.1
1938.5±0.8	0.2±0.1	2503.4±0.8	0.2±0.1
1959.1±0.5	0.6±0.1	2514.4±0.8	≈ 0.2
1968.3±0.7	0.2±0.1	2526.3±0.8	0.2±0.1
1974.4±0.5	1.4±0.2	2543.0±0.8	0.2±0.1
2000.4±0.7	0.3±0.1	2561.0±0.9	0.2±0.1
2011.3±0.8	0.2±0.1	2579.3±0.8	0.2±0.1
2015.9±0.5	1.3±0.2	2604.0±0.7	0.2±0.1
2013.0±0.9	≈ 0.1	2615.7±0.8	0.2±0.1
2030.3±0.9	≈ 0.1	2699.8±0.9	≈ 0.1
2061.3±0.8	0.2±0.1	2712.7±0.7	0.2±0.1
2086.9±0.9	≈ 0.1	2737.4±0.9	≈ 0.1
2090.9±0.8	0.2±0.1	2814.0±0.9	≈ 0.1
2097.3±0.8	0.2±0.1	2907.0±1.0	≈ 0.1
2103.6±0.7	0.4±0.1	2949.5±0.9	≈ 0.1
2129.8±0.6	0.5±0.1	2960.8±0.8	0.2±0.1
2140.0±0.5	1.3±0.2	3077.5±0.7	0.2±0.1
2157.6±0.7	0.4±0.1	3166.2±0.6	0.3±0.1
2175.4±0.8	0.2±0.1	3180.4±0.7	0.2±0.1
2192.1±0.6	0.3±0.1	3191.4±0.7	0.3±0.1
2210.0±0.5	0.0±0.1	3196.2±0.9	≈ 0.1
2231.5±0.5	0.9±0.1	3287.4±0.6	0.3±0.1
2250.0±0.8	0.2±0.1	3292.4±0.8	0.2±0.1
2258.8±0.7	0.3±0.1	3297.4±0.5	0.7±0.1
2310.5±0.8	0.2±0.1	3334.8±0.9	≈ 0.1
2337.0±1.0	≈ 0.1	3390.8±0.7	0.4±0.1

Table 2 (continued)

E_{γ} , keV	I_{γ} ^{d)}	E_{γ} , keV	I_{γ} ^{d)}
3400.4 \pm 0.6	0.3 \pm 0.1	3535.9 \pm 0.8	0.2 \pm 0.1
3417.5 \pm 0.7	0.3 \pm 0.1	3575.7 \pm 0.6	0.4 \pm 0.1
3436.2 \pm 0.6	0.2 \pm 0.1	3588.5 \pm 0.9	\approx 0.1
3445.2 \pm 0.8	0.2 \pm 0.1	3747.0 \pm 0.9	\approx 0.1
3517.8 \pm 0.9	\approx 0.1		

a) γ -ray transitions observed in ref. ^{b)}.

b) Placed in the decay scheme.

c) Double lines as concluded from the γ - γ coincidence measurements. These lines were twice placed in the decay scheme as a consequence of γ - γ coincidences.

d) Intensities are given per 100 decays (see text).

e) Values derived from the γ - γ coincidence measurements.

f) Annihilation radiation.

photometrically determined density (corrected for radius and film response). All results from the conversion electron measurements in the decays of ^{162}Yb , ^{162}Tm and ^{160}Tm are given in tables 1, 4 and 5, respectively. The multipolarities of the γ -ray transitions are deduced from a comparison of K-conversion coefficients, K/L₁ ratios and L- and M-subshell ratios with theoretical values of conversion coefficients computed by Hager and Seltzer ²⁶.

2.4. Gamma-gamma coincidence measurements

In order to place the observed γ -ray transition in the level schemes γ - γ coincidence measurements were performed with two Ge(Li) detectors of volumes of 22 and 25 cm³ with system resolutions of 5 keV for ^{60}Co . The resolving time of the coincidence system was about 170 ns.

Table 3 Energies and intensities of the γ -ray transitions in the decay $^{160}\text{Tm} (\beta^+) ^{160}\text{Er}$

E_{γ} , keV	I_{γ} ^{d)}	E_{γ} , keV	I_{γ} ^{d)}
KX (Er)	88 \pm 9	1102.7 \pm 1.2 ^{b)}	0.6 \pm 0.3
125.7 \pm 0.1 ^{a)}	34.7 \pm 5.0	1151.8 \pm 0.8 ^{b)}	1.1 \pm 0.3
264.0 \pm 0.1 ^{a)}	9.4 \pm 1.2	1249.1 \pm 0.6	2.8 \pm 0.4
(389.0 \pm 0.8) ^{b)}	0.7 \pm 0.3	1264.1 \pm 0.8	1.3 \pm 0.3
511.0 ^{c)}	2x(15 \pm 2)	1269.7 \pm 0.7	3.0 \pm 0.3
520.2 \pm 0.8	0.5 \pm 0.2	1340.5 \pm 1.0	0.5 \pm 0.2
527.0 \pm 0.8 ^{b)}	0.8 \pm 0.3	1372.5 \pm 0.5	8.6 \pm 0.7
548.4 \pm 0.8	0.6 \pm 0.3	1394.7 \pm 0.6	3.6 \pm 0.4
597.1 \pm 0.6	1.7 \pm 0.3	1409.4 \pm 1.0	0.7 \pm 0.3
617.5 \pm 0.6	1.6 \pm 0.3	1460.6 \pm 0.6	4.3 \pm 0.5
636.4 \pm 0.8 ^{b)}	0.8 \pm 0.3	1526.4 \pm 0.6	3.8 \pm 0.4
640.1 \pm 0.7	1.6 \pm 0.3	1536.6 \pm 0.8	1.1 \pm 0.2
665.0 \pm 0.8	0.8 \pm 0.3	1586.9 \pm 0.7	1.0 \pm 0.2
681.7 \pm 0.7	0.7 \pm 0.3	1768.5 \pm 0.8	0.8 \pm 0.2
728.5 \pm 0.5 ^{a)}	12.8 \pm 1.2	1801.1 \pm 1.0 ^{b)}	0.6 \pm 0.2
767.8 \pm 0.6	2.9 \pm 0.3	1862.6 \pm 0.9 ^{b)}	0.8 \pm 0.2
797.7 \pm 0.6	2.7 \pm 0.4	1894.4 \pm 1.1	0.9 \pm 0.3
854.4 \pm 0.5 ^{a)}	8.1 \pm 0.7	2065.5 \pm 0.5	1.1 \pm 0.3
861.4 \pm 0.5 ^{a)}	7.0 \pm 0.6	2123.4 \pm 0.8	1.1 \pm 0.3
882.0 \pm 0.6	2.2 \pm 0.3	2202.2 \pm 0.7 ^{b)}	1.9 \pm 0.3
985.5 \pm 0.7	0.9 \pm 0.3	2214.1 \pm 0.5 ^{b)}	1.1 \pm 0.3
1000.2 \pm 0.8	0.7 \pm 0.3	2403.9 \pm 0.9 ^{b)}	0.7 \pm 0.3
1007.7 \pm 0.6	2.5 \pm 0.3	2424.3 \pm 1.0 ^{b)}	0.8 \pm 0.3

a) γ -ray transitions observed in ref. ⁵⁾.

b) Not placed in the decay scheme.

c) Annihilation radiation.

d) Intensities are given per 100 decays (see text).

Table 4 The results of the conversion electron measurements of the γ -ray transitions in the decay $^{162}\text{Tm}(\beta^+)^{162}\text{Er}$

E_{γ} , keV	I_{β}	I_{K}	Multipolarity
102.00	17.3 ^{a)}	18.0 ^{a)}	E2
227.44	6.3	0.7	E2
571.0 ^{b)}	2.1 $\begin{cases} 0.4^{\text{c)}} \\ 1.7^{\text{c)}} \end{cases}$	≤ 0.02	(E2) ^{d)} (E1, E2) ^{e)}
672.2 ^{b)}	0.2 $\begin{cases} 4.5^{\text{c)}} \\ 1.7^{\text{c)}} \end{cases}$	0.035	(E2) ^{d)} (E1) ^{c)}
708.5 ^{b)}	5.7 $\begin{cases} 0.5^{\text{c)}} \\ 1.9^{\text{c)}} \end{cases}$	0.06	(E2) ^{d)} (M1) ^{c)}
900.4 ^{b)}	11.6 $\begin{cases} 0.5^{\text{c)}} \\ 4.8^{\text{c)}} \end{cases}$	0.05	(E2) ^{d)} (E2, M1) ^{e)}
1250.1	4.5	≤ 0.005	E1
1318.4	5.1	≈ 0.01	E2
1352.0	3.6	≤ 0.005	F1
1401.9	2.5	< 0.005	F1, (E2)

a) Normalization values.

b) Double lines as concluded from the γ - β coincidence measurements.

c) Values derived from the γ - β coincidence measurements.

d) Multipolarities assumed from the placement of these components of the double lines in the decay scheme were used for the calculation of the multipolarities signed by the symbol ^{e)}

All intensities are given per 100 decays (see text). The errors of the conversion electron intensities are of the order of 20%.

Experimental l-subshell ratios of the 102.00 and 227.44 keV transitions were determined to be $I_{111}^1/I_{111}^0 = 1.4/0.4$ and $I_{111}^1/I_{111}^0 = 0.00/0.12/0.1$, respectively.

Table 5 The results of the conversion electron measurements of the γ -ray transitions in the decay $^{160}\text{Tm}(\beta^+)^{160}\text{Er}$

E_{γ} , keV	I_{γ}	I_{K}	$I_{\text{L I}}$	$I_{\text{L II}}$	$I_{\text{L III}}$	Multi- polarity
125.7	14.7 ^{a)}	21 ^{a)}	2	10	0	E2
204.0	9.4	0.8	0.1	0.13	0.10	E2
354.4	8.1	0.04				E2
501.4	7.0	0.03				E2

a) Normalization values.

All intensities are given per 100 decays (see text). The errors of the conversion electron intensities are of the order of 20%.

Several digital windows were placed on the photopeaks and on the continuous background slightly above these peaks in order to correct the contribution of coincidence with the continuous distribution under the photopeaks. The coincidence spectra were simultaneously stored in a memory of maximum 24576 channels (for further details see ref. ²³⁾). Usually, measurements of 10 sources were added. All the results from the γ - γ coincidence measurements in the decays of ^{162}Tm and ^{160}Tm are summarized in tables 6 and 7. The coincidence data indicate that the peaks at 571.0, 672.2, 798.8 and 900.4 keV observed in the ^{162}Tm decay are double lines. The intensities of their components were evaluated on the basis of the coincidence measurement results.

2.5. Beta-gamma coincidence measurements

For the determination of the decay energies of ^{162}Tm and ^{160}Tm measurements of the positron spectra in coincidence with γ -rays, de-populating well established

low energy levels in the daughter nucleus, were performed [22]. A coincidence system consisting of a (64x4) cm³ NaI(Tl) γ -ray detector with system resolution of 9% for ¹³⁷Cs and Si(Li) β -detector of 100 mm² surface and 15 mm thickness with system resolution of 8 keV for the 975.6 keV electron line of ²⁰⁷Bi was used for the β - γ coincidence measurements. The resolving time of the coincidence system was 50 ns. The positron radiation feeding the 2⁺ states of the ground-state rotational band in ¹⁶²Er and ¹⁶⁰Er was measured in coincidence with the 102.00 and 125.7 keV transitions de-populating these states, respectively. For the correction of the contribution of coincidences with the continuous distribution under the peaks digital windows were also placed slightly above the peaks of these 2⁺ \rightarrow 0⁺ transitions. The coincidence spectra were simultaneously stored in two memories of 4096 channels. The energy calibration of the β -detector was performed with the conversion electron lines of ²⁰⁷Bi and the β -transitions of ¹⁴⁴Pr and ¹⁰⁶Rh. The β^+ -spectra corrected in the back-scattering effect of the detector with the aid of the β -transition of ¹³⁸Pr were analysed by Fermi-Curie Plots (for further details see ref. [22]). The endpoint energies of the positron spectra measured in coincidence with the 102.00 keV ¹⁶²Tm γ -rays and the 125.7 keV ¹⁶⁰Tm γ -rays were determined to be 3500 \pm 300 keV, 3700 \pm 500 keV, respectively.

3. Discussion

3.1. The ¹⁶²Yb decay scheme

The ¹⁶²Yb decay scheme proposed in refs. [1,2] is confirmed by the results of the present investigations (see fig. 4). The intensities of the population of the 163.36 keV level and the ground state by electron capture and positron decay were evaluated to be 77% and 22%, respectively. These values are in good agreement with the limit values of > 60% and < 40% derived by Goudsmit

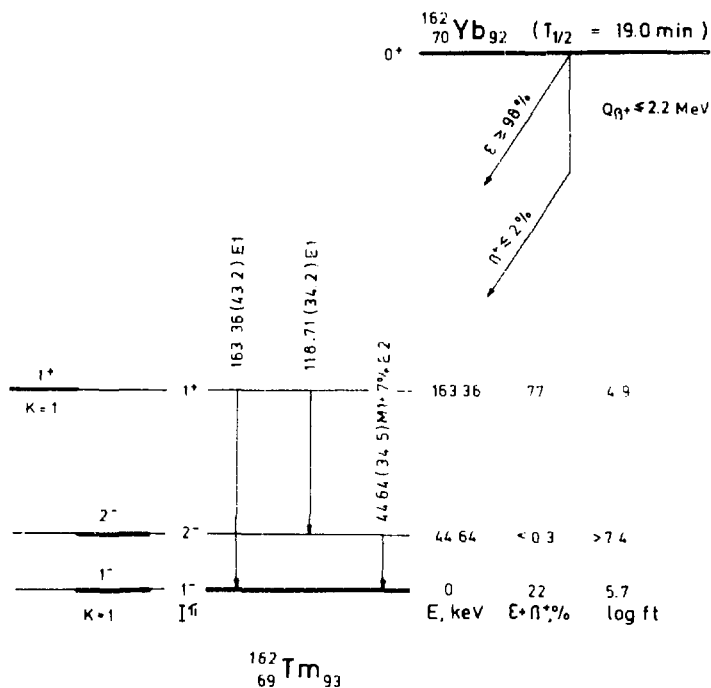


Fig. 4. The decay scheme of ^{162}Yb . Energies are given in keV, total intensities per 100 decays.

et al. /2/ only from the KX -ray intensity in the ^{162}Yb decay for the population of the 163.36 keV level and the ground-state, respectively. From the measured intensity of the annihilation radiation an upper limit of 2% was obtained for the β^+ -radiation in the ^{162}Yb decay. Using these values a lower limit of 36 was evaluated for the K -capture to positron ratio for the population of the

163.36 keV level. This K/β^+ ratio corresponds to an upper limit of the positron energy of about 950 keV for the allowed unhindered β -transition observed in refs. ^{1,2} to the 163.36 keV two-quasiparticle state $1^+, p 7/2^- [523] - n 5/2^- [523]$ which de-excite by two strong E1 transitions to the 1^- and 2^- member of the $K=1$ ground-state band. Thus the Q-value of ^{162}Yb was derived to be ≤ 2.2 MeV and limits for the $\log ft$ values given in fig. 4 can be calculated. This upper limit for the Q-value of ^{162}Yb is in agreement with the calculated ^{162}Yb Q-value ²⁷ of 2.3 MeV used in ref. ²⁷.

3.2. The ^{162}Tm decay scheme

The ^{162}Tm decay scheme based on our experimental results is shown in fig. 5. The level energies given in the present study are more precise than those in previous works (refs. ^{3,4-6}). For the calculation of the $\log ft$ values in fig. 5 a Q-value of 4.6 ± 0.3 MeV deduced from our β - γ coincidence measurements was used. This Q-value confirmed recently by Beetz et al. ²⁸ is in good agreement with the proposed Q-value of 4.8 MeV in ref. ⁵ and the calculated Q-value of 4.7 MeV in ref. ²⁷.

For the $\log ft$ values in fig. 5 only lower limits are given mainly as a consequence of intensive unplaced γ -rays with a total intensity of about 30%. The $\log ft$ values of the β -transitions to the 0^+ and 2^+ members of the ground-state rotational band in ^{162}Er (see fig. 5) confirm for the ^{162}Tm ground-state the 1^- character obtained from the measured spin $l=1$ (refs. ^{9,10}) and the ^{162}Yb decay studies ^{1,2}.

New levels at 1352.0, 1505.6 and 1572.7 keV were found in ^{162}Er in addition to the 0^+ , 2^+ and 4^+ members of the $K=0$ ground-state band, the 2^+ , 3^+ and 4^+ members of the γ -vibrational band, the 0^+ and 2^+ members of the β -vibrational band and two levels at 1420.3 and 1595.3 keV. Other ^{162}Er levels observed previously in the ^{162}Tm decay ^{5,6} were not confirmed.

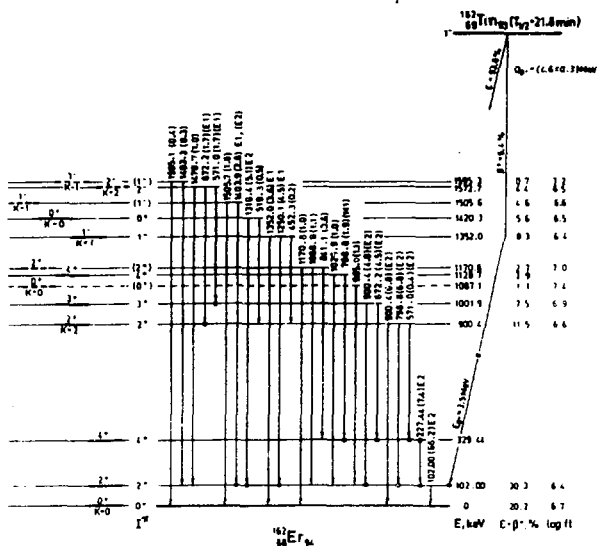


Fig. 5. The decay scheme of ^{162}Tm . Energies are given in keV, total intensities per 100 decays. Transitions the placement of which is strongly (weakly) supported by coincidences are marked by full (open) dots.

The $KI^{\pi} = 11^{-}$ character for the 1352.0 keV state was deduced from the $E1$ multipolarity of the strong γ -ray transitions to the first two members of the ground-state rotational band.

Spin and parity of the 1420.3 keV state were not known previously. For this state a $KI^{\pi} = 00^{+}$ assignment was derived from the $E2$ multipolarity of the 1318.4 keV transition to the 2^{+} member of the ground-state band and from the fact that a γ -ray transition to the ground-state itself was not observed.

The de-population mode of the 1505.6 keV level and the probable $E1$ multipolarity of the 1403.9 keV transition de-populating this level to the 2^{+} member of the ground-state band suggest the 1505.6 keV state to have a $KI^{\pi} = 11^{-}$ character.

The level at 1572.7 keV might be from its γ -de-population a $KI^{\pi} = 22^{-}$ state, although its interpretation as being the first excited rotational state of the 1505.6 keV state cannot be excluded.

The 1^{-} character of the 1595.3 keV state was tentatively proposed by Tjom and Elbek ⁴⁷. It is in agreement with the γ -de-population of this state.

Many high energy transitions in the ^{162}Tm decay (see fig. 2 and table 2) indicate a significant feeding of high-lying states. But from the available information their establishment on the level scheme is not unambiguous.

3.3. The ^{160}Tm decay scheme

The ^{160}Tm decay scheme constructed from the results of the present investigations is shown in fig. 6. The calculation of the $\log ft$ values is based on a Q -value of 4.9 ± 0.5 MeV obtained in β - γ -coincidence measurements. In addition to the ^{160}Tm ground-state spin $I = 1$ measured by Ekström et al. ⁴⁹ a 1^{-} character for the ground-state of ^{160}Tm can be deduced from the $\log ft$ values of the β -transitions to the 0^{+} and 2^{+} members of the $K = 0$ ground-state band (see fig. 6).

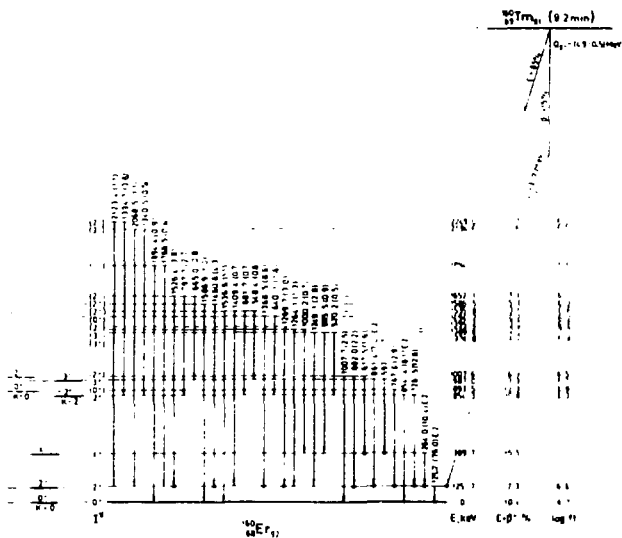


Fig. 6. The decay scheme of ^{160}Tm . Energies are given in keV, total intensities per 100 decays. Transitions the placement of which is strongly (weakly) supported by coincidences are marked by full (open) dots.

Table 6 Gamma-gamma coincidences observed in the decay
 $^{162}\text{Tm}(\beta^+)^{162}\text{Er}$

gated lines E_{γ_1} , keV	coincident lines E_{γ_2} , keV ($I_{\gamma}^{\text{coinc.}}$)
102.00	227.44 (180), 511.0 ^{a)} , 571.0 (40), 672.2 (100) ^{b)} , 798.8 (185), 900.4 (130), 1026.0 (30), 1250.1 (120), 1318.4 (100), 1403.9 (80)
227.44	571.0 (20), 672.2 (100) ^{b)} , 798.8 (40)
672.2	227.44 (45), 798.8 (100) ^{b)} , 900.4 (127)
798.8	227.44 (30), 511.0 ^{a)} , 672.2 (100) ^{b)}
900.4	511.0 ^{a)} , 571.0 (50), 672.2 (100) ^{b)}

a) Annihilation radiation.

b) Normalization values.

Except the 0^+ , 2^+ and 4^+ members of the ground-state band and the two levels at 854.3 and 987.0 keV reported by de Boer et al.¹¹ 12 new levels in ^{160}Er were observed. Spin and parity assignments of the levels at 854.3 keV (2^+) and 987.0 keV (3^+) are based on our conversion electron measurements and the de-population mode. Using the $\log ft$ values and the de-population modes spin and parity assignments of the other levels are tentatively given in fig. 6. The existence of the levels at 389.7, 854.3, 893.5, 987.0, 1007.6, (1395.4), 1494.2, 1586.5,

Table 7 $\beta^- \gamma$ coincidences observed in the decay $^{160}\text{Tm}(\beta^+)^{160}\text{Er}$

gated lines E_{J_1} , keV	coincident lines E_{J_2} , keV ($J_2^{\text{coinc.}}$)
125.7	264.0 (0 ⁺) ^a , 511.0 ^a , 728.5 (100) ^b , 767.8 (15), 861.4 (60), 882.0(17), 1269.7 (30), 1367.5 (67), 1490.6 (37), 1520.4 (33).
264.0	597.1 (60), 617.5 (100) ^b
728.5	511.0 ^a

^a) Annihilation radiation.

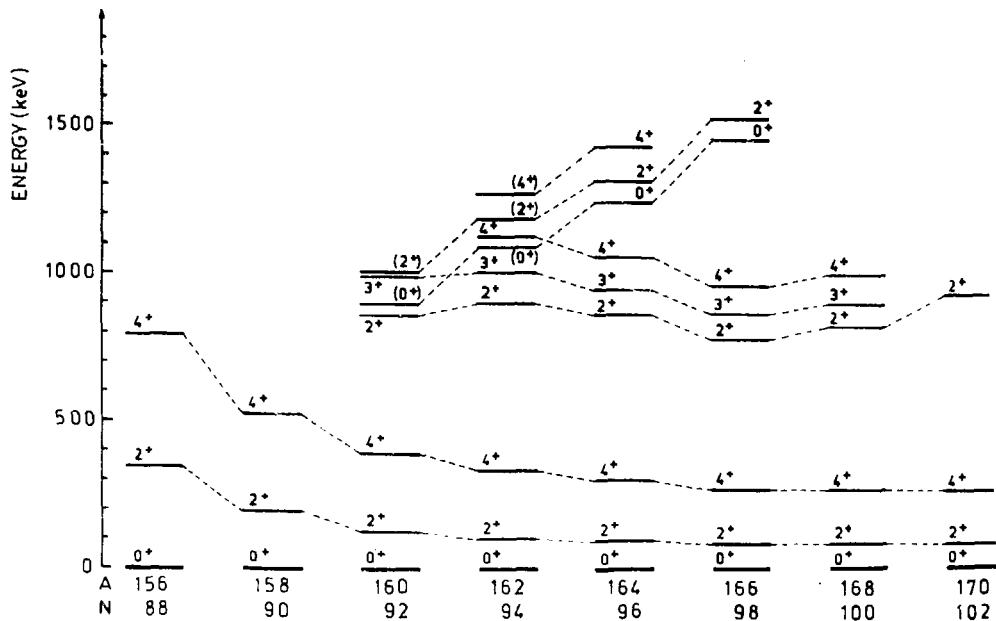
^b) Normalization values.

and 1652.1 keV is deduced from the coincidence measurements (see table 7). The other levels in fig. 6 are based on energy sum relations.

The states at 854.3 and 987.0 keV are interpreted as the first two members of the γ -vibrational band. Arguments supporting this interpretation are the $\log ft$ values, the rotational parameter, the de-population mode and the E2 multipolarity of the 854.4 and 861.4 keV transitions.

From the $\log ft$ values, the rotational parameter and the de-population mode the levels at 893.5 and 1007.6 keV could tentatively be explained as being the 0⁺ and 2⁺ members of the β -vibrational band.

The level energies of the β^- and γ -bands in ^{160}Tm are in good agreement with the energy level systematics of the low energy states in the even Er nuclei $^{152,154,156,158}\text{Er}$ in fig. 7.



25 Fig. 7. Energy level systematics on the low energy states in the even Er nuclei.

Recently a ^{160}Tm decay scheme has been published in a short report by Beetz et al. ³⁵ In general their results agree quite well with our published also previously ¹⁴⁻¹⁶. The ^{160}Tm Q-value was not measured by Beetz et al. ³⁵. Our proposed level scheme of ^{160}Er appears to be more complete.

It is a pleasure to thank Professor V.P. Dzhelepov, Dr. D. Netzband and Dr. L. Funke for their support. The valuable assistance of the synchrocyclotron staff of the JINR Dubna and of the electronics teams of the measuring centre of the LNP JINR is gratefully acknowledged.

References

1. K.Ya. Gromov, T.A. Islamov, G. Ischakov, M. John, H. Tyrroff, S.A. Usmanova, V.I. Fominych, E. Herrmann, H. Strusny. Proc. of the Conf. on Nucl. Spectroscopy and Nucl. Structure, Kiev, 1972, p. 132.
2. P.F.A. Goudsmit, F.W.N. de Boer, B.J. Meijer, M. Bogdanov. Nucl. Phys., A196, 362 (1972).
3. O. Saethre, S.A. Hjorth, A. Johnson, S. Jagere, H. Ryde, Z. Szymanski. Nucl. Phys., A207, 486 (1973).
4. P.O. Tjøm, B. Elbek. Nucl. Phys., A107, 385 (1968).
5. A.A. Abdurazakov, G. Bayer, K.Ya. Gromov, H.M. Islamova, T.A. Islamov, S.M. Kamalchodjaev, H. Strusny. Proc. of the Conf. on Nucl. Spectroscopy and Nucl. Structure. Leningrad, 1970, p. 117.
6. Y.Y. Chu. Phys. Rev., C4, 642 (1971).
7. M. Neiman, D. Ward. Ann. Rep. of the Lawrence Rad. Lab., Berkeley, California (UCRL 18667), p. 59.
8. F.W.N. de Boer, P.F.A. Goudsmit, P. Koldewijm, B.J. Meijer. Radiochimia Acta, 13, 118 (1969).
9. C. Ekstrom, M. Olmats, B. Wannberg. Nucl. Phys., A170, 649 (1971).
10. C. Ekstrom. I.-L. Lamm. Physica Scripta, 7, 31 (1973).
11. C. Ekstrom, I. Lindgren, H. Nyqvist, A. Rosen, K.-E. Edelhö. Phys. Lett., 26B, 146 (1968).
12. G. Beyer, K.Ya. Gromov, H.-U. Siebert, T.A. Islamov, G. Ischakov, M. John, F. Molnar, H. Tyrroff, S.A. Usmanova, E. Herrmann, H. Strusny, M. Jachim. Proc. of the Conf. on Nucl. Spectroscopy and Nucl. Struct., Tbilisi, 1973, p. 90.

13. G.Beyer, K.Ya.Gromov, H.-U.Siebert, T.A.Islamov, E.Herrmann, H.Strusny, M.Jachim. Proc. of the Conf. on Nucl. Spectroscopy and Nucl. Struct., Charkov, 1974, p. 120.
14. R.Arlt, K.Ya.Gromov, H.-U.Siebert, T.A.Islamov, M.John, H.Tyroff, S.A.Usmanova, E.Herrmann, H.Strusny. Proc. of the Conf. on Nucl. Spectroscopy and Nucl. Structure, Kiev, 1972, p. 129.
15. R.Arlt, G.Beyer, K.Ya.Gromov, H.-U.Siebert, T.A.Islamov, M.John, F.Molnar, H.Tyroff, S.A.Usmanova, E.Herrmann, H.Strusny, M.Jachim. Proc. of the Conf. on Nucl.Spectroscopy and Nucl. Structure, Tbilisi, 1973, p. 86.
16. R.Arlt, G.Beyer, K.Ya.Gromov, H.-U.Siebert, T.A.Islamov, M.John, F.Molnar, H.Tyroff, S.A.Usmanova, E.Herrmann, H.Strusny, M.Jachim. Proc. of the Conf. on Nucl.Spectroscopy and Nucl. Struct., Charkov, 1974, p. 166.
17. Z.Malek, G.Pfrepper. Dubna Report, 12-4013 (1968).
18. G.Musiol, V.I.Raiko, H.Tyroff. Dubna Report, R6-4487 (1969).
19. G.Beyer, E.Herrmann, A.Ipotrowski, V.J.Raiko, H.Tyroff, Nucl.Instr. and Meth., 96, 437 (1971).
20. B.K.Preobrazhensky, O.M.Lilova, A.N.Dobronravov, E.D.Teterin. Zhurnal Neorg. Chim., 1, 2294 (1956).
21. W.A.Kotschetkov, N.A.Lebedev, A.F.Novgorodov, W.A.Chalkin. Radiochimiya, 6, 73 (1964).
22. R.Arlt, G.Winter, S.V.Medved, G.Musiol, A.N.Sinaev, S.A.Usmanova, D.Fromm, N.A.Tschistov, H.Strusny. Pribory i Technika Eksperimenta, 6, 71 (1972).
23. V.S.Aleksandrov, F.Duda, O.I.Elisarov, G.P.Zhukov, G.I.Sabiyakin, S.Seider, I.Zvolsky, E.T.Kondrat, S.V.Lysenko, V.I.Prichodko, V.G.Tischin, V.I.Fominych, M.I.Fominych, V.M.Zupko-Sitnikov. Izv. Akad. Nauk SSSR (ser. fiz.), 34, 69 (1970).
24. G.J.Nijgh, A.H.Wapstra, R. van Lieshout. Nuclear Spectroscopy Tables, North-Holland Publishing Company-Amsterdam, 1959.
25. A.A.Abdurazakov, A.I.Achmadjanov, K.Ya.Gromov, T.A.Islamov, S.M.Kamalchodjaev, M.K.Prokofjev. Dubna Report, R6-4363 (1969).
26. R.S.Hager, E.C.Seltzer. Nucl. Data, A4, 1 (1968).
27. A.H.Wapstra, N.B.Gove. Nucl.Data Tables, 9, 267 (1971).
28. R.Beetz, F.W.H. de Boer, P.F.A.Goudsmit, P.Kolde-wijn, I.Konijn, B.J.Meijer, W.L.Posthumus, A.v.d.Schaaf. IKO Progress Report 72/73, p. 24.

29. F.W.N. de Boer, P.F.A.Goudsmit, P.Koldewijn, B.J.Meijer. Nucl.Phys., A169, 577 (1971).
30. C.W.Reich. Nucl.Phys., A159, 181 (1970).
31. G.E.Keller, E.F.Zganjar, J.J.Pinjian. Nucl.Phys., A129, 481 (1969).
32. Y.Yoshizawa, B.Elbek, B.Herskind, M.C.Olesen. Nucl.Phys., 73, 273 (1965).
33. R.Graetzer, E.M.Bernstein. Phys.Rev., 129, 1772 (1963).
34. A.Abdumalikov, J.Adam, J.Vrsal, V.Gnatovich, K.Gromov, M.Kuznetsova, V.Kuznetsov, J.Liptak, V.Morozov, G.Musiol, J.Urbanec, M.Finger, V.Chumin. Dubna Report,R6-3343 (1967).
35. R.Beetz, F.W.N. de Boer and P.F.A.Goudsmit, IKO Progress Report 73/73, p. 24.

Received by Publishing Department
on June 6, 1974.